Chapter 14

ESD Knitted Fabrics from Conductive Yarns Used as Protective Garment for Electronic Industry

Gabriela Telipan, Beatrice Moasa, Elena Helerea, Eftalea Carpus, Razvan Scarlat and Gheorghe Enache

Additional information is available at the end of the chapter

http://dx.doi.org/10.5772/intechopen.69843

Abstract

Nowadays, interest in protection against electrostatic discharge (ESD), regarded as an important issue, is still growing. ESD may lead to serious economic losses and can also be hazardous to humans. In zones where substances with low values of ignition energy occur, ESD may involve a high risk of fire or explosion. Protective clothing is used to reduce the risk of electrostatic discharge (ESD) in electronics industry as well as in explosive atmospheres. In the manufacturing process of electronic products, significant percentage-related failures due to ESD phenomena that occur on the production line, especially where they are not installed systems and rigorous protection rules, are still recorded. Protective clothing with antistatic properties is designed to prevent the transfer of electrical charge from human operator to electronic device during the manufacturing process. In this chapter, a study was conducted about the electrical parameters representative for the control of electrostatic discharges as well as the surface and volume resistivity by applying the current absorption-resorption method and parameters of charge decay using the standardized induction method on several knitted conductive fabrics with carbon yarn. Current absorption-resorption method is applied for the first time in research under antistatic and dissipative fabrics.

Keywords: ESD garments, electrostatic discharge, absorption-resorption current method, surface, volume resistivity

1. Introduction

Textile materials that provide comfort, antimicrobial, antiallergenic, and anti-stress protection or shielding for working people in environments with high-risk factors are increasingly required to protect consumers' health, prevent diseases, and reduce environmental impact [1, 2].

A new concept has been created to transform the passive role of textile materials to an active role with all their influence for industry and consumers.

To keep up with the strategy for upgrading the textile companies, the researchers' main objective was to achieve high-performance technologies with low impact on the environment and human body and promotion of raw materials using superior hygienic, antibacterial, antiallergenic, and protective properties for people who work in hazardous environments.

In modern electrostatic discharge (ESD) protection systems, protective clothing is provided to prevent accidental ESD events caused by an operator and which can partially or totally destroy electronic devices from polychlorinated biphenyl (PCBs). Neither currently these problems are not completely eliminated. Thus, researchers have identified the need for protective clothing to have two properties at the same time but this is possible only if the garment is made of two layers.

The first property is linked to the need for a low conductivity of material for limiting electric charge processes and transferring related and the second property is linked to the need for an increased conductivity to facilitate dissipation of electrical charges processes on the material [3]. In order to prevent the occurrence of electrostatic fields which produce and induce electric charges in materials [4, 5], protective clothing and work surfaces should have electrostatic shielding properties [6]. ESD processes are dependent on temperature and humidity [5].

The conductive fabrics have been considered from their electromagnetic shielding and anti-electrostatic properties for various applications in the defense, and electrical and electronic industries [7–11].

The surface resistivity is a principal parameter which determines the ESD protection applications [12]. Generally, the synthetic fibers used for textiles fabrics have an electrical insulation character, with a surface resistivity about 10^{15} Ω/□. This value of surface resistivity is very higher for anti-electrostatic and electromagnetic shielding applications.

Many researches show that to obtain good and efficient anti-electrostatic material, a surface resistivity in the range of (10^{9}–10^{12}) Ω/□ is necessary, and for statically dissipative material, the surface resistivity values must be in the range of (10^{4}–10^{9}) Ω/□ [13].

In order to improve the electric conductivity of textiles, different techniques are applied, for example, the introduction in textile material of conductive yearns, carbon or metal [13–15], or treatment with conductive polymer, polyaniline, polypyrrole, poly(3,4-ethylenedioxythiophene)-polystyrene sulfonate PEDOT–PSS [13, 16, 17].

The research conducted by authors in the field of technical textiles was on knitted bilayer that provides good protection from accidental electrical discharges on the dielectric layer and a drainage of accumulated charges through conductive layer. An image of the bilayer concept is illustrated in **Figure 1** [18].

The external layer is predominantly dissipative and it provides protection to short circuit and the limitation of the electrostatic energy that can be dissipated to the work environment, and the internal layer is predominantly conductive, providing controlled drainage of cumulated

http://dx.doi.org/10.5772/intechopen.69843

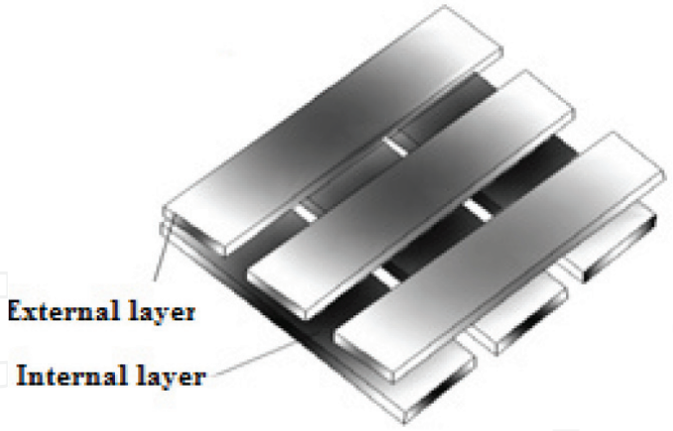

Figure 1. The bilayer concept of ESD fabric.

electrostatic charges. Also, an additional requirement for the internal layer is to provide comfort to the user.

The principal objective of our study consists in the development of a comparative analyzer for several ESD garments with carbon-conductive thread used for electronic industry and the characterization regarding their anti-electrostatic properties. The absorption-resorption measurement method is applied for obtaining the charge decays and surface and volume resistivities, as main parameters of ESD static and dissipative properties of garments.

2. ESD characteristics and measurement methods

2.1. Surface and volume electrical resistivities and the absorption-resorption current method

The procedure for determining the surface and volume resistivities is based on the current absorption-resorption method. This method was earlier applied to highlight the aging processes of insulating materials [19], but it can significantly also characterize the electrostatic charging-discharging processes in ESD protection materials.

The procedure consists of applying a DC voltage V on a sample, disposed in the measuring cell (with three electrodes, e.g., Keithley 8009 cell) and recording the values of current intensities to coupling source (absorption currents) and then to decoupling source (resorption currents).

Absorption current i_a is determined by applying a continuous voltage V across the capacitor (measuring cell), having as dielectric the material sample with conductivity σ and permittivity ε, an absorption current will flow through the circuit.

The absorption current intensity $i_a(t)$ is variable in time t and has specific components:

$$i_a(t) = i_0(t) + i_p(t) + i_{ch}(t) + I_\sigma \tag{1}$$

where: $i_0(t)$ is the charging current of vacuum capacitor, $i_p(t)$ is the polarization current, $i_{ch}(t)$ is the space charge current, and I_σ is the conduction current [20, 21].

The charging current of vacuum condenser $i_0(t)$ decreases rapidly to zero, as the transitional regime is exceeded. Expression of this current is dependent on the time of variation, and the electric field intensity is

$$i_0(t) = \varepsilon_0 . \frac{\Delta E}{\Delta t} . S \tag{2}$$

where ε_0 is the permittivity of vacuum, S is the electrode surface, and E is the electric field intensity.

Polarization current $i_p(t)$ is determined by the polarization processes occurring in the material. Depending on the mechanism of polarization (electronic, orientation, interfacial/dishomogeneity polarizations), this current tends to zero after reaching permanent regime of DC power.

Space charge current $i_{ch}(t)$ stems from the movement of electrically charged structural units (ions, impurities, etc.) under the action of the electric field intensity E established in the material. The electric space charges can occur due to technological processes, in thermal degradation, electrical stresses, and so on. The space charge current can distort readings for conduction current intensity I_σ values. Therefore, it is necessary to determine the time constant τ feature for transitory regime of current flowing.

Steady-state regime is characterized by conduction current I_σ, given by the free electric charges flow under the action of the applied electric field and showing no change value in time. Usually, steady-state regime is considered to be achieved after a time of (3–5)τ, where τ is the time constant of the circuit. So, the measurement of conduction current intensity should be taken only after achieving the steady-state regime [22], and the average value of I_σ is obtained taking into account the measured values in steady-state regime of current flowing.

Depending on the arrangement of the measuring electrodes, the value of the volume current intensity I_V or the value of the surface current intensity I_S is determined and, as in the voltammeter method, the volume and surface resistivities are obtained.

When this no longer applies to voltages and the electrodes that are short-circuited, the discharging process begins, and in the material sample a transient current, named resorption current, flows. The intensity of resorption current $i_r(t)$ depends on time t and has specific components too:

$$i_r(t) = i_d(t) + i_{dp}(t) + i_{ch}(t) \tag{3}$$

where $i_d(t)$ is the discharge current, $i_{dp}(t)$ is the depolarization current, and $i_{ch}(t)$ is the space charge current.

A simplification of the time dependence of the absorption and the resorption current intensities in a polar dielectric is shown in **Figure 2**.

http://dx.doi.org/10.5772/intechopen.69843

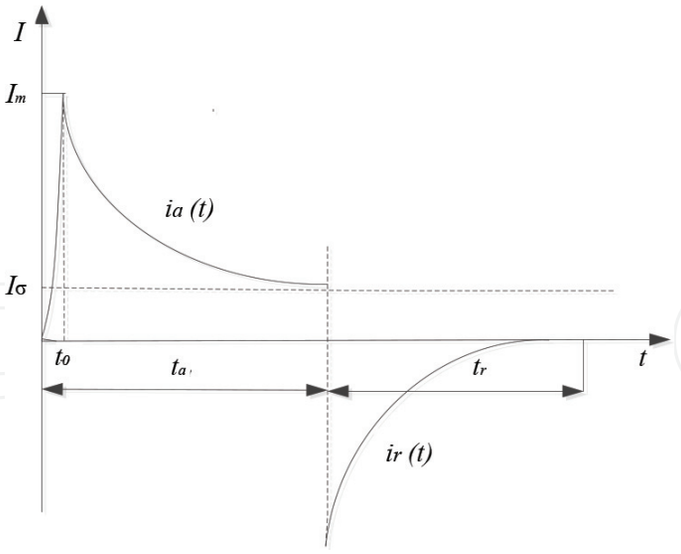

Figure 2. Time dependence of the absorption and resorption currents in a polar dielectric.

The absorption current decreases asymptotically toward the steady state, due to dielectric polarization and the sweep of mobile charges to the electrodes. For materials of high resistivity (up to 10^{13} Ωm, and 10^{12} Ω/□) the steady state is reached in several minutes, hours, and days. For these materials, the time dependency of the volume resistivity is taken into account.

For an antistatic material—surface resistivity is in the range of (10^{9}–10^{12}) Ω/□ [13]—the steady-state regime in general is reached within 1 min (**Figure 3**), and the resistance is then determined after this time of DC voltage supplying.

Comparison of **Figures 3** and **4** shows that the steady-state regime in antistatic polymers is established earlier than in polar dielectrics, the absorption current slope $i_a(t)$ is steeper and the resorption current $i_r(t)$ also has a steep slope.

For dissipative materials with surface resistivity of the order of 10^{6}–10^{10} Ω/□, the wave forms of absorption and resorption currents differ from those of antistatic or insulating materials [23–25].

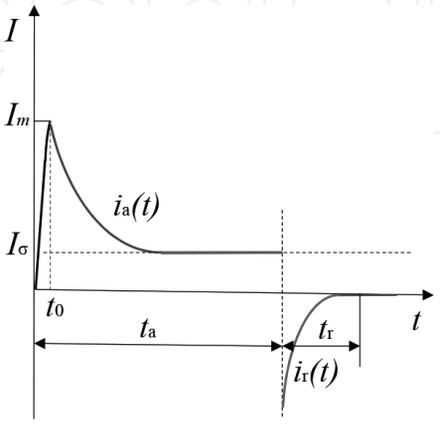

Figure 3. Time dependence of the absorption and resorption currents in antistatic polymers.

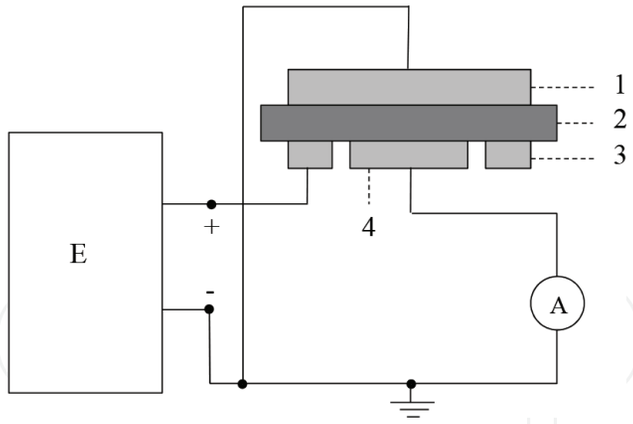

Figure 4. Scheme for measuring surface resistivity: (1) upper electrode; (2) sample material; (3) guard ring; and (4) the measuring electrode.

In materials, the free electric charges—both conduction processes—in volume of material and on the surface—are present, even at low electric field stresses.

Based on these processes, the volume and surface resistivities can be good indicators of ESD antistatic comportment of materials: the surface resistivity of material can characterize the ability of a material to dissipate electrostatic charges; the volume resistivity of a material is useful for evaluating the relative dispersion of a conductive additive throughout the polymer matrix, and it can related to electromagnetic shielding effectiveness in certain conductive fillers.

To determine the volume resistivity ρ_V and surface resistivity $\rho_{S,}$ with absorption-resorption current method, the same scheme is used, described in standard SR HD 429 S1 CEI 60093 [26]. The measurement principle of the method is similar to the volt-amperometric method, where single difference positions guard ring electrode.

Measurement scheme for determining the surface resistivity is shown in **Figure 4**.

In this case, the applied voltage reaches the sample through the guard ring, the read signal by the ammeter coming from the measuring electrode.

Surface resistivity is defined as the quotient of a DC electric field applied between two electrodes on a surface of a specimen and the filiform current density of the current flowing between the electrodes at a given time of electrification:

$$\rho_s = \frac{E}{J_s} \tag{4}$$

where E is the electric field intensity, in V/m, and J_S is the surface current density, in A/m.

The surface resistivity shall be calculated with the following relation:

$$\rho_s = \frac{R_s \cdot p}{g} = K_s \cdot \frac{U}{I_s} \tag{5}$$

where is the surface resistivity, in Ω/□, R_S is the surface resistance, in Ω, p is the effective perimeter of the guarded electrode, in m, g is the distance between the electrodes, in m, U is

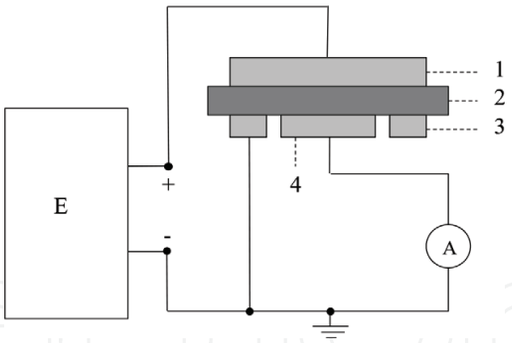

Figure 5. Scheme for measuring the volume resistivity: (1) upper electrode; (2) sample; (3) guard ring; and (4) measuring electrode.

the applied voltage, in V, and I_s is the surface current intensity, in A. The coefficient K_s is calculated in the function of the geometry of measurement cell and the particular electrode arrangement.

Measurement scheme for determining the volume resistivity is shown in **Figure 5**.

In this case, the applied voltage reaches the sample through the upper ring, the signal read by the ammeter coming from the measuring electrode.

Volume resistivity is defined as the quotient of a DC electric field strength applied to a material specimen disposed between two electrodes and the current density J_v of the current flowing between the electrodes at a given time of electrification:

$$\rho_v = \frac{E}{J_v} \tag{6}$$

where E is the electric field intensity, in V/m, and J_v is the volume current density, in A/m^2.

The volume resistivity shall be calculated with the following relation:

$$\rho_v = \frac{R_v \cdot A}{h} = \frac{K_v}{h} \cdot \frac{U}{I_v} \tag{7}$$

where ρ_v is the volume resistivity, in Ωm, R_v is the volume resistance, in Ω, A is the effective area of the guarded electrode, in m^2, h is the average thickness of the specimen, in m, U is the applied voltage, in V, I_v is the volume current intensity, in A. The coefficient K_v, given by the effective area A of guard electrode, is calculated in the function of the geometry of measurement cell and the particular electrode arrangement.

In the case of the measuring cell Keithley, the measuring electrode and guard ring are at the bottom of the circuit arrangement.

2.2. Parameters of charge decay and measurement methods

A way to characterize the rate of dissipation of electrostatic charge of garment materials is to study charge decay. Charge decay is the process of migration of charge across or through a

material leading to a reduction of charge density or surface potential at the point where the charge was deposited.

To monitor the mobility of electrostatic accumulated charges, two methods of measurement are used [28]. In both methods, the charge is monitored by the observation of the electrostatic field it generates and this is done using non-contacting field-measuring instruments. The principal difference between the methods is the technique used to generate the electrostatic charge: (1) triboelectric charging, when the material specimen is in contact with a special rod, rubs together and subsequently separates. The electrical field strength from the charge generated on the test material is observed and recorded using an electrostatic field meter connected to a graphical recording device; (2) induction charging, which involves a field electrode, placed near the surface of a specimen, and which is energized with high voltage. If the specimen contains mobile electric charges, the charge of opposite polarity to the field electrode is induced on the specimen. Induced charge on the test material influences the net field, and this effect is measured and registered with a field-measuring probe, positioned above the test surface.

In **Figure 6**, the scheme for determining the discharge time of the material specimens, which are charged through electric induction [18], is shown. The main components of the measuring stand are signal generator (G), electronic voltmeter (VE), oscilloscope (OSC), sample (1), support sample (2), field electrode (3), measurement electrode (4), and guard ring (5) [18].

A step high voltage is applied on field electrode. By electrical induction, in the sample the electrical charges are separated and an electric field of intensity E_R is generated in the surrounding area. The electric field generated by electric induction is compared to the electric field generated by the electric field in the absence of a sample.

The electric field strength indicated on the recording device in the absence of the test specimen has maximum value and could be obtained with the electric flux law:

$$E_{max} = \frac{Q}{\varepsilon_0 \cdot A} \tag{8}$$

where E_{max} is the intensity of the electric field near the measurement electrode in the absence of the specimen, in V/m; ε_0 = 8.855 pF/m is the vacuum permittivity; A is the effective area of the measurement electrode; Q is the accumulated electric charge in the specimen, respectively, in measurement electrode, obtained with the relation:

Figure 6. Installation for testing the capacity to dissipate electrical charge for textiles.

$$Q = C \cdot U \tag{9}$$

In relation (9), C is the capacity of the condenser without the specimen, and U is the voltage applied at the terminals. Capacity C is obtained usually through measurement with bridge measurement systems.

The electric field strength E_R indicated on the recording device with the test specimen in the measuring position is also registered in time.

The half-decay time t_{50} is defined as the interval of time in which the electric field intensity decreases to the value $E_R/2$. This parameter indicates the electric field strength decay to $E_R/2$ and is an indicator for classification of textiles as static or dissipative.

The shielding factor S is defined by the relationship between E_{max} and E_R and is calculated as: [18, 27, 28]

$$S = 1 - \frac{E_R}{E_{max}} \tag{10}$$

The advantage of using the induction method of charging the specimen is that it allows to determine both parameters—half-decay time and shielding factor, which characterize the ability to dissipate electrical charge of any antistatic or dissipative textile.

3. Experimental determinations

3.1. Conductive fabrics specimens manufacturing and examination

In order to assure the bilayer structure, the chosen knitting structures were plated plain jersey and plated rib. The knitting technology presumed electronic flatbed knitting machines (Stoll, 7E and 12E gauge). The bilayer knitted variants were made in plaited structures, with parallel evolution of two or more yarns with strictly determined relative position as a result of their settling at different angles (plaiting yarn V at an angle smaller than ground yarn F). In case of jersey structure, the plaiting yarn V appears on the foreground on the front and the ground yarn F, on the foreground on the back of the fabric. In case of rib structure due to alternating of front-back wales, both the plaiting yarn and the ground yarn will be present on the foreground, on each side of the fabric, **Figure 7**.

The used yarns were:

Base yarn: Nm 50/3, 100% cotton; Nm 30/2, 100% wool.

Conductive yarns, as follows:

- for inner layer: 75% cotton + 25% epitropic yarn (Nm 34/1 carbon coated polyester)—named yarn type 2.
- for outer layer: multifilament yarn made from surface-saturated nylon with carbon particles—named yarn type 5.

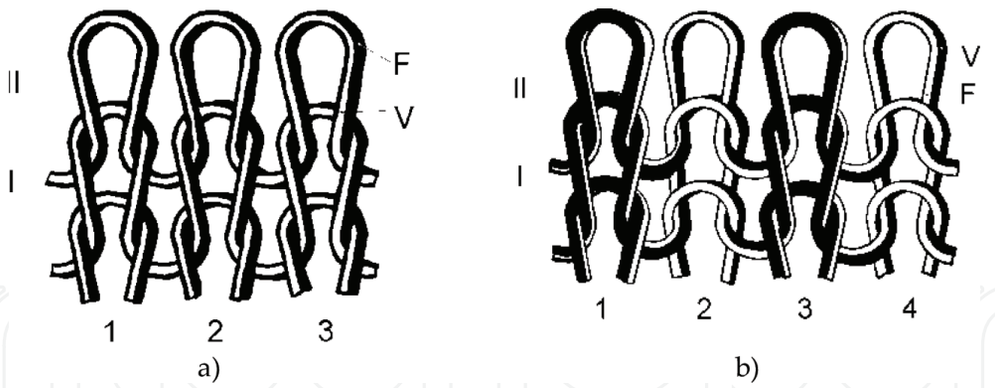

Figure 7. Structural representation of plaited: (a) plain jersey structure; (b) plaited rib structure.

Figure 8 shows the image for ESC knitted fabrics supposed to experiments.

In order to characterize the nine knitted fabric samples, complete sets of analyses have been realized and conducted for the following parameters: weight (g/m^2), density (wales/10 cm, rows/10 cm), thickness (mm), air permeability ($l/m^2/s$), water vapor permeability (%), thermal conductivity (mW/mK), and thermal resistance (m^2KW). Experimental data are presented in **Table 1**, and in **Figure 9**, few images with analyzed samples are shown.

In **Table 2**, the composition and structure of knitted fabrics for surface and volume electrical resistivity test and for electrostatic shielding factor are presented.

From the data presented in **Table 2**, it can be observed that the percentage of conductive wire varies depending on the number of yarns and their composition.

3.2. Measurement setups

A. Surface and volume resistivity measurement have a setup composed by Electrometer Keithley 6517A (1–1000V), with Keithley 8009 measure cell, and computer with control soft and data processing shown in **Figure 10** [30].

Figure 8. ESD knitted fabrics.

http://dx.doi.org/10.5772/intechopen.69843

Sample code	Weight [g/m^2]	Density		Thickness [mm]	Air permeability [l/m^2/s]	Water vapor permeability [%]	Thermal resistance [m^{2}K/W]	Thermal conductivity [mW/mK]
		[rows/10 cm]	[wales/10 cm]					
P10	597	47	81	1.62	374.4	36.2	0.03269	49.55
P11	589	47	82	1.66	395.0	35.9	0.04444	37.35
P12	634	47	75	1.74	401.4	34.0	0.03395	51.25
P20	562	47	69	1.65	601.0	34.8	0.04099	40.25
P19	603	46	69	1.66	647.6	30.06	0.03567	46.55
P14	828	36	59	3.58	576.6	28.5	0.05732	62.45
P13	878	36	59	3.61	609.8	32.4	0.05726	63.05
P17	802	34	60	3.53	800.8	29.5	0.07801	45.25
P18	846	33	59	3.57	872.2	28.6	0.07786	45.85

Table 1. The characteristics of knitted samples [29].

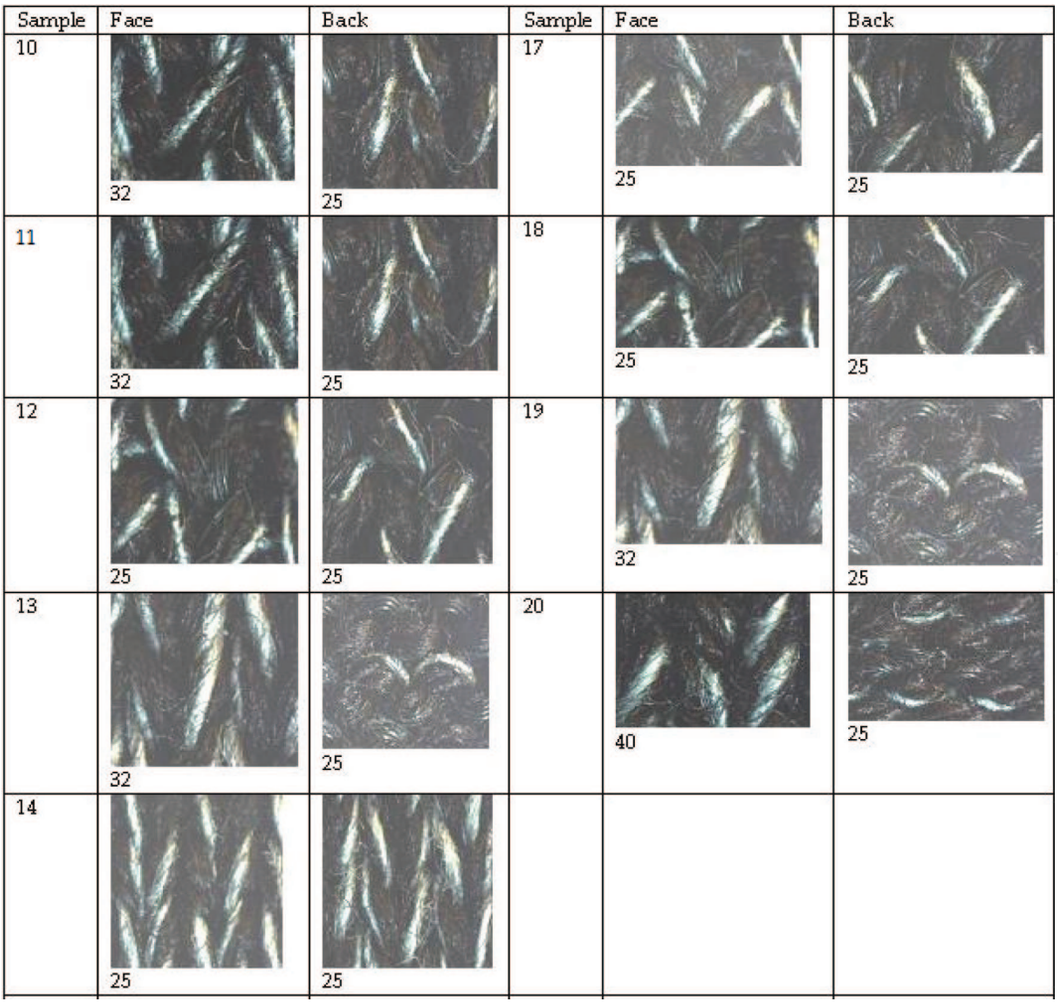

Figure 9. Optical images for knitted fabrics. The parameters 25, 32, and 40 represent the image magnitude.

Knitted structure	Knitted fabric		Percent of conductive yarn [%]	Indicator
	Outer layer/front side of fabric	Inner layer/back side of fabric		
Plaited plain jersey	One cotton yarn + one yarn type 2*	One cotton yarn + one yarn type 5**	4.5	P10
		One cotton yarn + 2 yarns type 5	6.0	P11
		One cotton yarn + 3 yarns type 5	7.5	P12
	One wool yarn + one yarn type 2	One wool yarn + 2 yarns type 5	6.0	P20
		One wool yarn + 3 yarns type 5	7.6	P19
Plaited rib	One cotton yarn + one yarn type 2	One cotton yarn + 2 yarns type 5	6.0	P14
		One cotton yarn + 3 yarns type 5	7.5	P13
	One wool yarn + one yarn type 2	One wool yarn + 2 yarns type 5	6.0	P17
		One wool yarn + 3 yarns type 5	7.5	P18

* Yarn type 2 content 75% cotton + 25% epitropic yarn (Nm 34/1 carbon coated polyester).
** Yarn type 5 content multifilament yarn made from surface-saturated nylon with carbon particles.

Table 2. Composition and structure of knitted fabrics for surface and volume electrical resistivity test and electrostatic shielding factor [28].

Figure 10. Stand for surface and volume resistivity measurements.

The characteristics of the measurement cell is as follows: (1) the size surface coefficient is K_s = 53.37 Ω/□ (distance between electrodes is d = 0.3175 cm, and the average diameter D = 5.3975 cm); (2) the size volume coefficient is $K_v = 20.25802 \times 10^{-4}$ cm^2, where ρ_v is in [Ω·cm], g is the average thickness of the sample in [cm]; U is the applied voltage, in [V], I_V is the volume conduction current, in [A].

The application time of the signal is t = 20 s and the read time after cutoff signal is t = 10 s. The total measuring time was 30 s. In the early 1920s, DC voltage was applied, and for the remaining 10 s the signal was cut off and the remaining currents were measured on surface material.

The minimum value of applied voltage to textile samples is 1 V and the maximum value applied varies from sample to sample; limitation criteria for applied voltage are given by electrometer. Keithley electrometer used can highlight the current of fA-mA (10^{-15}–10^{-3}) order.

From the values obtained for surface conduction current, values of steady state, within the time interval (12–18) s, have been extracted. This was done similarly for volume conduction current.

The values of surface and volume resistivity are calculated using relations (5) and (7).

The average values and mean-square dispersion values have been calculated and corrections have been done: for dispersions greater than 5%, the erroneous values have been eliminated.

In all the samples, it was observed that after about 12 s, the values of absorption current intensities are stabilized.

B. Time decay of electric charge and shielding factor evaluation has a setup built in accordance with standard SR EN 1149-3:2004 used. The image of measurement stand is shown in **Figure 11** [18, 28].

The test facility includes the following elements:

1. Electrostatic generator for inducing electric charge in the sample.
2. Base support.
3. Flange support.
4. Electrodes for the measurement of electric field intensity.
5. Stretching system of textile samples.

The apparatus used for electric induction charging is an electrostatic machine type, and for measurement, the following are used: Bridge ESCORT ELC-132A for measuring capacity; Oscilloscope-type Fluke 1968; kilovoltmeter Fluke HP 0-30 kV. The procedure for experimental determination of the half-decay time and the shielding factor using the induction charging method has been applied. For obtaining the electric field intensity value without fabric sample

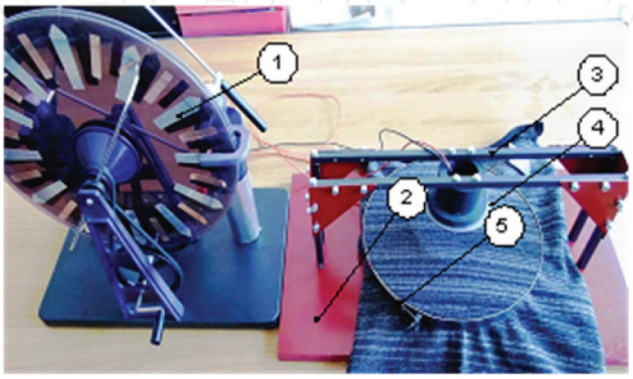

Figure 11. Image of the ESD setup for assessing the ability to dissipate electrical charge.

E_{max} and with sample E_R, the following data have been obtained: (1) from generator, a voltage pulse is applied, the measured value is U_0 = 6.9 kV; (2) capacitance between the electrodes without the sample is C_0 = 59 pF; (3) the value of the accumulated electric charge, calculated by relation (9), is Q_0 = 407.1 nC; (4) electric field intensity value determined by relation (8) is E_{max} = 119.54 kV/cm. The electrodes have a diameter of 70 mm and section A = 38.465 cm.

The procedure for establishing the electric field intensity with sample between the electrodes is the following: (1) electrostatic generator induces electric field in a sample fixed on support; (2) the voltage value is recorded using an electronic voltmeter VE; and (3) the capacity of the sample system is measured using the bridge ESCORT ELC-132A.

4. Results and discussion

4.1. Surface and volume resistivity

The authors for each weaving technique have chosen a representative sample of the material. For vanish glad-weaving technique, the sample P11 experimental determinations are analyzed, and for vanish patent-weaving technique the sample P14 results are analyzed. The two samples have the same layer of the surface and the same type of conductor wire.

4.1.1. Textile sample P11

The image of P11 is shown in **Figure 12**.

For different values of DC voltage *U* applied to the sample, listed in **Table 3**, the average values of surface absorption current intensity of sample P11 in the steady-state regime are listed.

In **Figure 13**, the time dependences of the surface absorption current intensities for P11 sample, for different DC applied voltages, are shown.

For different values of DC voltage *U* applied to the sample, listed in **Table 4**, the average values of volume absorption current intensity of sample P11 in the steady-state regime are listed.

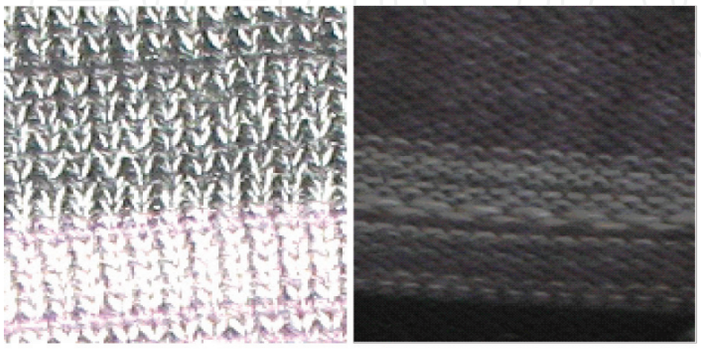

Figure 12. Macroscopic image of P11 bilayer sample: (a) face and (b) back.

A. Voltage between 1 and 5 V					
U [V]	1	2	3	5	
$I_{S\ med}$ [A]	3.2005E − 06	7.0300E − 06	1.0572E − 05	1.7705E − 05	
ρ_s [Ω/□]	1.6678E + 07	1.5186E + 07	1.5147E + 07	1.5075E + 07	
B. Voltage between 8 and 25 V					
U [V]	8	10	15	20	25
$I_{\sigma\ med}$ [A]	3.0106E − 05	5.1182E − 05	8.9558E − 05	1.3911E − 04	2.9869E − 04
ρ_s [Ω/□]	1.4159E + 07	1.0429E + 07	8.9406E + 06	7.6524E + 06	4.4678E + 06

Table 3. Average values of surface absorption current intensity and surface resistivity for P11 sample.

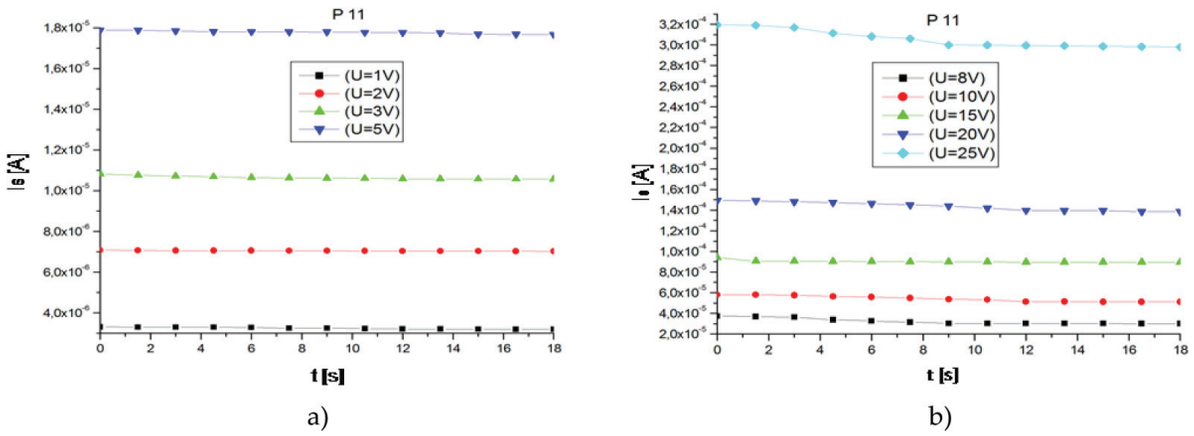

Figure 13. The time variation of surface absorption currents intensity for P11 sample, for DC applied voltages: (a) voltage between 1 and 5 V; (b) voltages between 8 and 25 V.

U [V]	1	2	3
I_{med} [A]	6.7346E − 05	1.5310E − 04	2.6073E − 04
ρ_v [Ω·cm]	2.6323E + 06	2.3158E + 06	2.0398E + 06

Table 4. Average values of volume absorption current intensity and volume resistivity for P11 sample.

In **Figure 14**, the time dependences of the surface absorption current intensities for P11 sample, for different DC applied voltage, are shown.

4.1.1.1. Discussions

Data in **Table 3** show that the values of the measured surface current intensities increase with increasing the applied voltage. The order of magnitude of currents measured is between 10^{-6}A for an applied voltage of 1 V and 10^{-4} A for an applied voltage of 25 V.

Surface resistivity varies with voltage values having a tendency to decrease with the increase in the applied voltage. The order of magnitude for surface resistivity is between (10^6–10^7) Ω/□ depending on the voltage applied. This sample has static dissipative behavior.

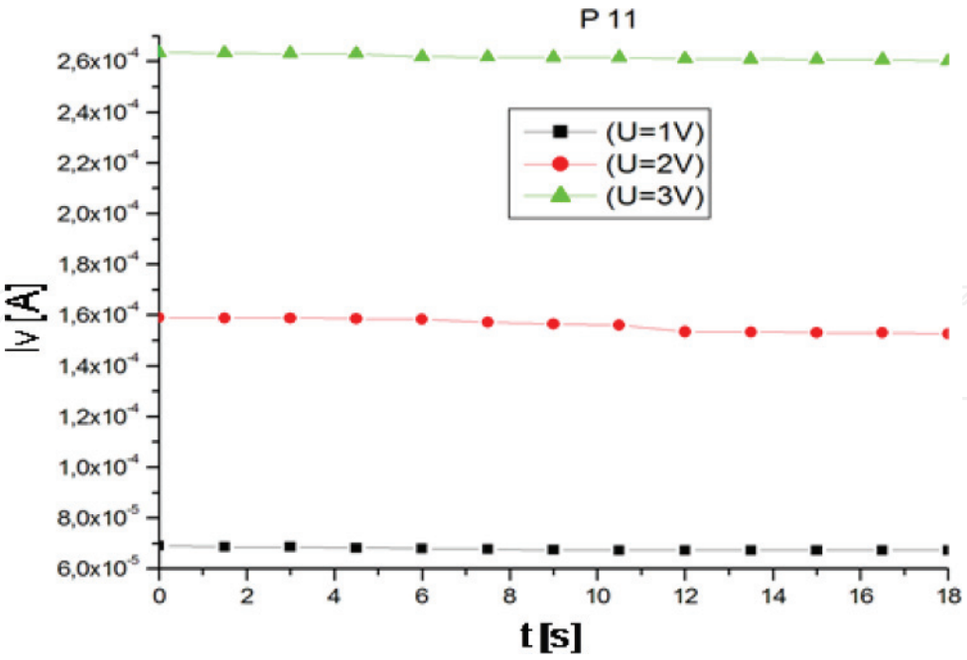

Figure 14. The time variation of volume absorption current intensity for P11 sample for DC applied voltages between 1 and 5 V.

Data in **Table 4** show that the order of magnitude of the volume absorption current is of 10^{-5} A for an applied voltage of 1 V and reach the values of 10^{-4} A for an applied voltage of 3 V.

Volume resistivity value decreases with the increasing applied voltage as in the case of surface resistivity. The order of magnitude for volume resistivity is 10^{6} Ω·cm.

4.1.2. Textile sample P14

The image of P14 is shown in **Figure 15**.

For different values of DC voltage *U* applied to the sample, listed in **Table 5**, the average values of surface absorption current intensity of sample P14 in the steady-state regime are

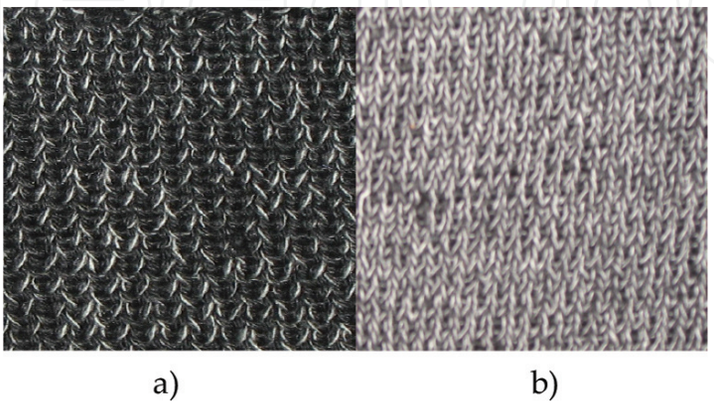

Figure 15. Macroscopic appearance of sample bilayer P14: (a) face and (b) back.

U [V]	1	2	3
I_{med} [A]	2.8207E − 04	6.6364E − 04	1.0680E − 03
ρ_s [Ω/□]	1.8924E + 05	1.6087E + 05	1.4994E + 05

Table 5. Average values of surface absorption current intensity and surface resistivity for P14 sample.

U [V]	1	2
I_{med} [A]	4.0038E − 04	1.4890E − 03
ρ_v [Ω·cm]	4.0224E + 05	2.1632E + 05

Table 6. Average values of volume absorption current intensity and surface resistivity for P14 sample.

listed. In **Table 6**, the average values of volume absorption current intensity of sample P14 in the steady-state regime are presented.

In **Figures 16** and **17**, the time dependences of the surface and volume absorption currents intensities for P14 sample, for different DC applied voltage, are shown.

4.1.2.1. Discussions

Data in **Table 5** show that the values of the surface measured current intensities increase with the increasing applied voltage value. The order of magnitude for surface measured current is between 10^{-4} A for an applied voltage of (1–2) V and 10^{-3} A for an applied voltage of 3 V.

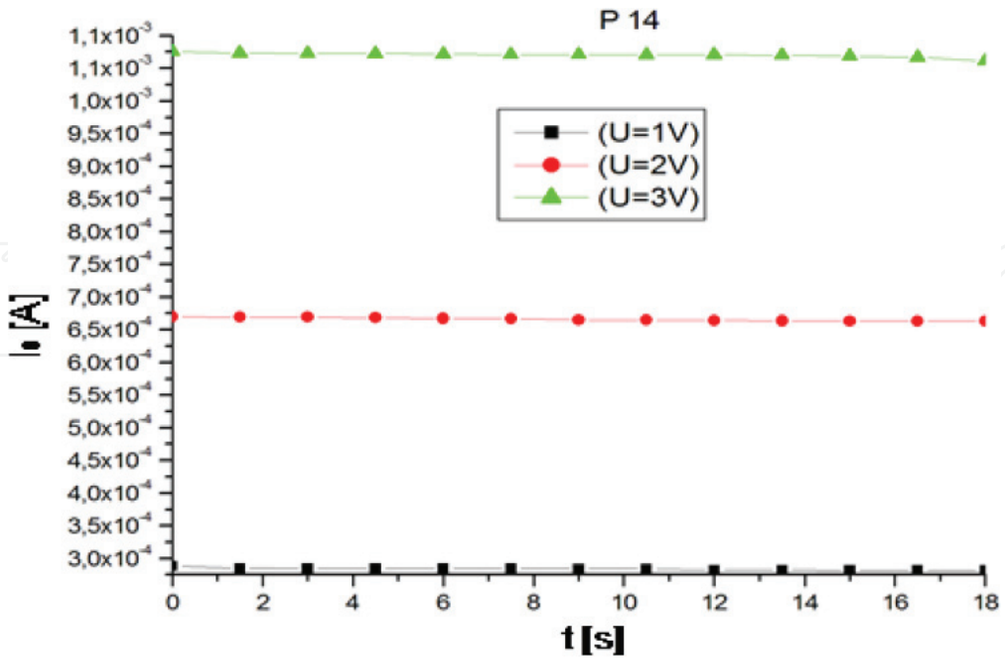

Figure 16. The time variation of surface absorption current intensity for P14 sample, for DC applied voltages between 1 and 3 V.

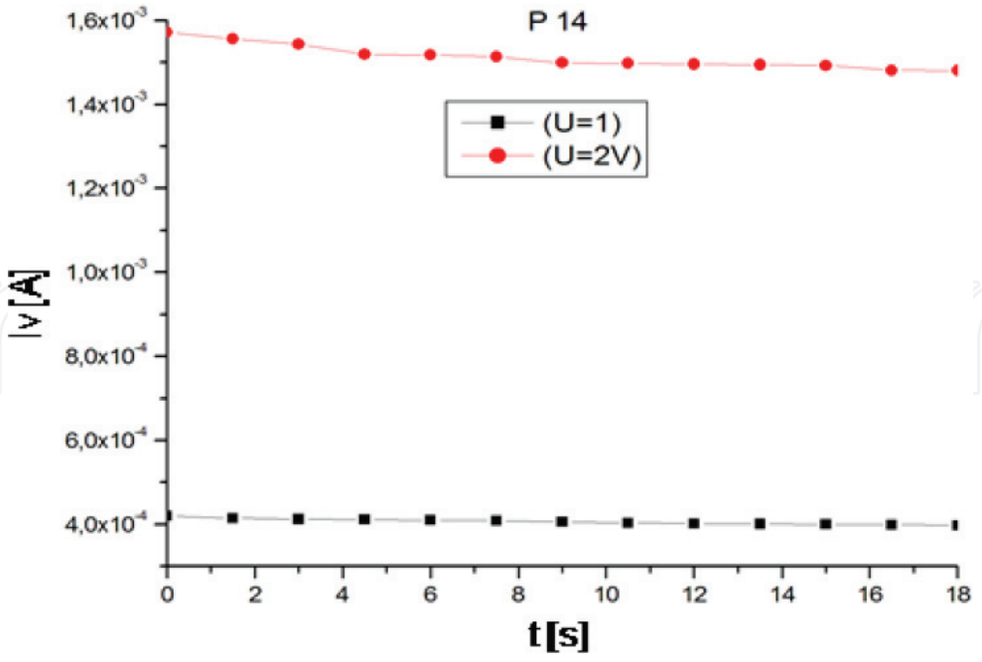

Figure 17. The time variation of volume absorption current intensity for P14 sample, for DC applied voltages between 1 and 2 V.

Surface resistivity decreases with increasing applied voltage, and the order of magnitude for surface resistivity is 10^5 Ω/□. This sample does not belong to the category of electrostatic dissipative materials ($\rho_s < 10^6$ Ω/□).

Data in **Table 6** show that the order of magnitude for volume measured current is 10^{-4} A corresponding to an applied voltage of 2 V. For voltage greater than 2 V, pico-ammeter cannot measure volume absorption currents for sample P14. Volume resistivity value decreases with the increasing applied voltage as in case of surface resistivity, and the order of magnitude of volume resistivity is 10^5 Ω·cm.

Analyzing the composition in terms of the two textile weaving techniques, it can be concluded with certainty that the technique of weaving plaited plain jersey is suitable for making electrostatic discharge protection clothes.

Plaited rib-weaving technique is not appropriate for these types of protective clothing. Resistivity values of surface and volume are not suitable for static dissipative properties of materials rather static conductive [31].

4.2. Charge decay and shielding factor

Experimental results obtained for capacity *C*, voltage *U*, electric charge on the fabric *Q*, electric field intensity E_R, half time decay of electric charge, and shielding factor are presented in **Table 7**. A comparative analysis regarding the half-decay time and shielding factor is shown in **Figure 18**, for the nine textile samples.

http://dx.doi.org/10.5772/intechopen.69843

Sample number	Sample code	C [pF]	U [kV]	Q [nC]	E_r [kV/cm]	E_0 [kV/cm]	t_{50} [ms]	S
1	P10	32	37	1184	346.9	260.1	100	0.72
2	P11	41	30	1230	360.3	240.2	100	0.7
3	P12	40.5	20	810	237.3	158.2	700	0.81
4	P18	40.5	19	770	225.6	150.4	550	0.82
5	P17	41.5	20	830	243.2	182.3	60	0.8
6	P19	40.3	21	846	247.8	162.2	250	0.8
7	P20	41.2	27	1112	325.8	217.2	700	0.73
8	P14	41.6	17	707.2	207.2	155.4	80	0.83
9	P13	41	30	1230	360.3	270.2	250	0.7

Table 7. Half-decay time and shielding factor for textile samples obtained with induction charging method [28].

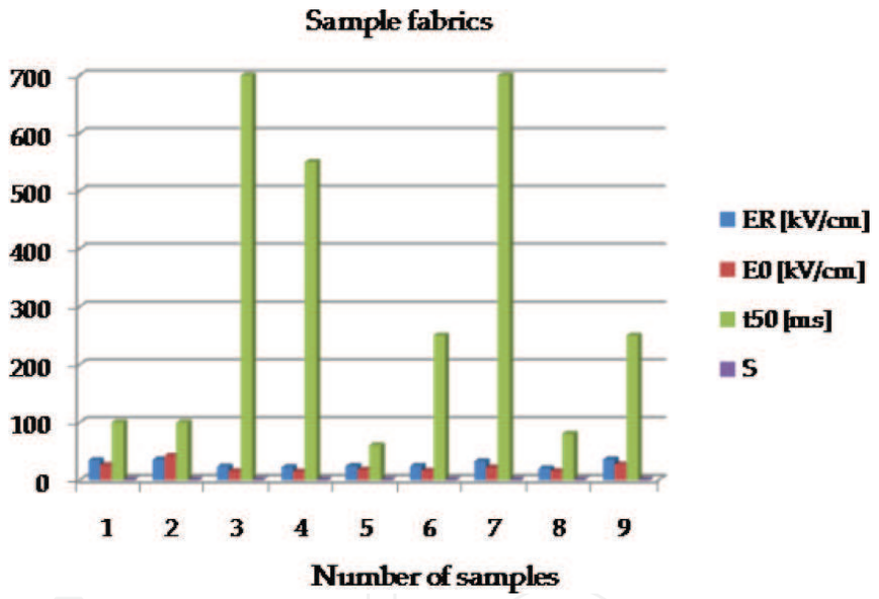

Figure 18. Graphical representation of parameters E_R, E_0, and t_{50}.

Half-decay time t_{50} and the corresponding value of electric field intensity E_0 are obtained from wave form signal on the oscilloscope. The shielding factor S for textile samples is determined based on relationship (10).

4.2.1. Discussions

Samples *5* (P17) and 8 (P14) presents the best values for time decay of electric charge and have shielding factors between 0.8 and 0.7. Samples *1* (P10) and 2 (P11) have values for time decay of electric charge of 100 ms and shielding factor 0.72 and 0.7, respectively. Samples *6* (P19) and *9* (P13) have time decay of electric charge of 250 ms and shielding factor of 0.8 and 0.7,

respectively. Sample 4 (P18) have time decay of electric charge 550 ms and shielding factor 0.82. Samples 3 (P12) and 7 (P20) have time decay of electric charge 700 ms and a shielding factor of 0.81 and 0.73, respectively. In terms of mitigating the electric field intensity, samples 3 (P12) and 7 (P20) have the lowest attenuation compared to other samples.

According to standard SR EN-1149-5:2008, all analyzed samples can be used to manufacture protective clothing, with the following observations: (1) for materials that do not have electrostatic shielding effect, $E_R = E_{max}$; (2) for materials with electrostatic shielding effect, $E_R < E_{max}$; (3) if $E_R < E_{max}/2$ is considered that $t_{50} < 0.01$ s; and (4) if value $E_{max}/2$ is reached in 30 s, $t_{50} > 30$ s is considered.

Samples 5 and 8 show the best times of time decay of electric charge <100 ms and have shielding factor 0.8 and 0.83, respectively. The composition of sample 5 (P17) is one wool yarn + one yarn type 2 for the outer layer/front side of the fabric and one wool yarn + two yarns type 5 for the inner layer/back side of the fabric. The composition of sample 8 (P14) is one cotton yarn + one yarn type 2 for the outer layer/front side of the fabric and one cotton yarn + two yarns type 5 for the inner layer/back side of the fabric. Yarn type 5 is made of nylon filament at the surface saturated with carbon particles.

Both samples were obtained by plaited rib knitted structures, have 6% percentage of conductive yarn, and have the same number of yarns type 5 in composition which distinguishes them as the base yarn.

The authors consider that the fabric with plaited rib-knitted structures together with the type of conductive yarn and the number of conductive yarns used (max. 2) offers the most efficient protection for time decay of electric charge.

The difference of value for electric field intensity (with sample) and time discharge of electric charge may be due to natural yarn structure.

5. Conclusions

The ESD equipment development was supposed to choose a knitted bilayer structure that can provide good protection from accidental electrical discharges on the dielectric layer and a drainage of accumulated charges through conductive layer.

The presence of the yarn type 2 on the front side determines the performance improvement by using the yarns types 3 and 5 for all knitting configuration; knitting structure does not significantly influence the ability of electrostatic discharge.

The limits of variation for water vapor permeability are between 28.5 and 42.5%, statistical events that agglomerate into optimal zone indicate the presence of the cotton yarn in rib structure. Air permeability causes sensations of warm and cool of clothing products, the best value being obtained by the samples 10, 11, 12 (374–400 l/m^2/s), characterized by the presence of cotton yarn and conductive yarn element from nylon filament surface saturated with carbon particles.

Simple electrical measurements, like two-point and four-point DC measurements, reveal the good electrical behavior of the yarn and fabric of the analyzed samples, when containing carbon-covered yarns. The measured resistances are in the M□-range and are sufficient to avoid electrical charge buildup in the fabric.

Analysis of physical-mechanical and functional characteristics indicates appropriate values for chosen knitting structure designed for ESD protection equipment.

Technical textiles have multiple applications which make possible to conduct further researches to obtain smart textiles.

Determination procedures for evaluating specific performance of textile and their calcification as static or dissipative are surface resistivity, volume resistivity, speed decay of electric charge and shielding factor, and time decay of electric charge which are additional parameters to assess these materials.

From determinations conducted for surface resistivity to samples described in **Table 1**, two aspects stand out, namely (a) if the percentage of conductive yarns increases, these fabrics become more conductive reaching surface resistivity values less than materials with dissipative properties ($\rho_s < 10^6$ Ω/□); (b) the textile structure (plain jersey and rib) influences the value of surface resistivity due to the presence of air in the textile structure, which makes the knitted samples with plaited rib structure to provide a higher conductivity than the samples with plaited plain jersey structure.

Also, when the voltage applied increases the value of current intensity, thus currents of the order of 10^{-3} A were highlighted. This aspect is not negligible in the case of higher voltages that may arise in case of real electrostatic discharges.

From determinations conducted for volume resistivity, it appears that the applied voltage values are lower and conduction processes in material are more intense than to surface. However, there are samples with volume resistivity of the order of 10^7–10^6 Ω·cm (P11, P12, P19, and P20).

From determinations conducted for time decay of electric charge and electrostatic shielding factor, three aspects stand out, namely (a) plaited rib structures offer the lowest times of decay of electric charge good and good electrostatic shielding coefficients; (b) the number of conductive yarns type 5 (filaments from nylon saturated at the surface with carbon) should not exceed two yarns (6% of conductive yarn) because at a greater number of conductive yarns intensive conducting processes can occur; (c) the aspects mentioned earlier must be correlated with the values obtained for surface and volume resistivity in order to make a complex analysis closer to actual needs and requirements of ESD protection systems.

Acknowledgements

This work was supported by a grant of the Romanian National Authority for Scientific Research, CNDI – UEFISCDI, project PCCA 179 – 2012 "ESD protective garments made with core conductive fibers knitted in double layer."

The authors also gratefully thank the staff of ELMAT Lab from the Polytechnic University of Bucharest for their support in the realization of some of the measurements, especially Prof. M. Dumitran.

Author details

Gabriela Telipan[1]*, Beatrice Moasa[2], Elena Helerea[2], Eftalea Carpus[3], Razvan Scarlat[3] and Gheorghe Enache[4]

*Address all correspondence to: gabriela.telipan@icpe-ca.ro

1 National Institute for Electrical Engineering ICPE CA, Bucharest, Romania

2 Transilvania University of Braşov, Braşov, Romania

3 The National Research & Development Institute for Textiles and Leather, Bucharest, Romania

4 TANEX SRL, Bucharest, Romania

References

[1] Agarwal BJ, Agarwal S. Integrated performance textiles designed for biomedical applications. In: Proceedings of International Conference on Biomedical Engineering and Technology IPCBEE. Vol. 11. Singapore: IACSIT Press; 2011. pp. 114-119

[2] Bahadir SK, Jevsnik S. Mint: Optimization of hot air welding process parameters for manufacturing textile transmission lines for e-textiles applications: Part I: Electroconductive properties. Textile Research Journal. 2017;**87**(2):232-243. DOI: https://doi.org/10.1177/0040517516629140

[3] Paasi J, Nurmi S, Kalliohaka T, Coletti G, Gustavino F, et al. Electrostatic testing of ESD protective clothing for electronics industry. In: Proceedings of Electrostatics Conference; 23–27 March; Edinburg. 2003. pp. 239-246

[4] Ardeleanu AS, Verejan A, Donciu C. Study regarding the knitting parameters in 3D textiles shields implementation. Mint: Acta Electrotehnica. 2010;**51**(2):128-131

[5] Helerea E, Moasa B, Ciobanu A. Analysis of electrostatic environment and discharge models. In: Proceedings of the IEEE International Conferences Applied Theoretical Electricity; 25–27 October 2012. Craiova: IEEE; 2012. pp. 1-4

[6] Baumgartner G. Consideration for developing ESD garment specifications. ESD TR 05-00 Report. ESD Association; 2000

[7] Chen HC, Lee KC, Lin JH, Koch M. Comparison of electromagnetic shielding effectiveness properties of diverse conductive textiles via various measurements techniques. Mint: Journal of Materials Processing Technology. 2007;**192–193**:549-554. DOI: https://doi.org/10.1016/j.jmatprotec.2007.04.023

[8] Ceken F, Pamuk G, Kayacan O, Ozkurt A, Ugurlu SS. Electromagnetic shielding properties of plain knitted fabrics containing conductive yarns. Mint: Journal of Engineered Fibers and Fabrics. 2012;**7**(4):81-87

[9] El-Newashy RF, Saad MA, Turky GM. Integration of conductive yarns into fabric by stitching. Mint: Journal of American Science. 2012;**8**(3):213-217

[10] Lemaire P. Forced Corona Method for the Evaluation of Fabrics with Conductive Fibres. Available from: http://estat.vtt.fi/publications/lemaire_poster.pdf

[11] Thilagavathi G, Raja ASM, Kannaian T. Nanotechnology and protective clothing for defence personnel. Mint: Defence Science Journal. 2008;**58**(4):451-459

[12] Rubeziene V, Baltusnikait J, Zuravliova SV, Sankauskaitea A et al. Development and investigation of electromagnetic shielding fabrics with different electrically conductive additives. Mint: Journal of Electrostatics. 2015;**75**:90-98. DOI: https://doi.org/10.1016/j.elstat.2015.03.009

[13] Chena HC, Lee KC, Lin JH, Kochc M. Comparison of electromagnetic shielding effectiveness properties of diverse conductive textiles via various measurement techniques. Mint: Journal of Materials Processing Technology. 2007;**192–193**:549-554. DOI: https://doi.org/10.1016/j.jmatprotec.2007.04.023

[14] Varnaite S, Katunskis J. Influence of washing on electric charge decay of fabrics with conductive yarns. Mint: Fibres and Textiles in Eastern Europe. 2009;**17**(5):69-75

[15] Hecht DS, Hu L, Gruner G. Electronic properties of carbon nanotube/fabric composites. Mint: Current Applied Physics. 2007;**7**:60-63. DOI: https://doi.org/10.1016/j.cap.2005.09.001

[16] Knittel D, Schollmeyer E. Electrically high-conductive textiles. Mint: Synthetic Metals. 2009;**159**:1433-1437. DOI: https://doi.org/10.1016/j.synthmet.2009.03.021

[17] Neelakandan R, Madhusoothanan M. Electrical resistivity studies on polyaniline coated polyester fabrics. Mint: Journal of Engineered Fibers and Fabrics. 2010;**5**(3):25-29

[18] Moaşa B, Helerea E, Ignat M, Telipan G. Experimental research on dissipative textile structures. In: Proceedings of the IEEE International Conference on Optimization of Electrical and Electronic Equipment OPTIM; 22–24 May 2014; Cheile Gradistei. Brasov: IEEE; 2014. pp. 155-160

[19] Dumitran LM, Bădicu L, Noţingher PV, Tănăsescu G. Premize pentru elaborarea unei metode de evaluare a stării de degradare a sistemelor de izolaţie ale transformatoarelor de putere pe baza curenţilor de absorbţie/resorbţie [Internet]. 2009. Available from: http://midmit.elmat.pub.ro/media/sec/LUCRARE%20Bran%202010_6ro.pdf

[20] Noţingher PV, Stancu C, Dumitran LM, Noţingher PP, Rakowska A, Siodla K. Influence of the ageing state of insulation systems on absorption/resorption currents. Mint: Revue Roumaine des SciencesTechniques – Serie Électrotechnique et Énergétique. 2008;**53** (2):163-177

[21] Stancu C, Noţingher PV. Influence of the surface defects on the absorption/resorption currents in polyethylene insulations. Mint: Scientific Bulletin of the Polytechnic University of Bucharest, Series C. 2010;**72**(2):161-170

[22] Dumitran LM. Electrical Insulation Systems (Sisteme de izolaţie electrică). Printech; 2008. 266 p

[23] Al-Saleh MH, Sundararaj U. A review of vapor grown carbon nanofiber/polymer conductive composites. Mint: Carbon. 2009;**47**:2-22. DOI: https://doi.org/10.1016/j.carbon.2008.09.039

[24] ASTM 257-14. Standard Test Methods for DC Resistance or Conductance of Insulating Materials

[25] Drake N. Polymeric Materials for Electrostatic Applications. Rapra Technology Ltd.; 1996. 168 p

[26] ***SR HD 429 S1 CEI 60093. Methods of Test for Volume Resistivity and Surface Resistivity of Solid Electric Insulating Materials. 2002

[27] ***SR EN 1149-3:2004,. Protective clothing—Electrostatic properties—Part 3: Test methods for measurement of charge decay

[28] Telipan G, Ignat M, Cătănescu L, Moaşa B. Electrostatic discharge testing of several ESD protective textiles used in electronic industry. In: Proceedings of the IEEE Electrical and Power Engineering International Conference and Exposition on (EPE); 16–18 October 2014; Iaşi: IEEE; 2014. pp. 602-605

[29] Carpus E, Vizileanu E, Scarlat R, Donciu C, Bonfert D, Popa A et al. Investigation of two-layer knitted structures with conductive fibres content. Mint: Industria Textila. 2014;**65** (3):145-152

[30] ***Keithley. Manual for the Use of the Electrometer Keithley 6715 A

[31] Moasa B. Contributions on Immunity Assessment of Equipment to Electrostatic Discharges [Internet]. 2015. Available from: http://webbut.unitbv.ro/teze/rezumate/2015/rom/MoasaCostelaBeatrice.pdf